https://doi.org/10.5194/egusphere-2025-762
Preprint. Discussion started: 7 March 2025
© Author(s) 2025. CC BY 4.0 License.

A Study of the Dependence between Soil Moisture and Precipitation in different Ecoregions of the Northern Hemisphere

Shouye Xue[a] and Guocan Wu [a*]

[a] *State Key Laboratory of Earth Surface Processes and Resource Ecology, Faculty of Geographical Science, Beijing Normal University, Beijing, 100875, China*

[*] *Corresponding author*: Guocan Wu, gcwu@bnu.edu.cn

https://doi.org/10.5194/egusphere-2025-762
Preprint. Discussion started: 7 March 2025
© Author(s) 2025. CC BY 4.0 License.

Abstract

Soil moisture plays a critical role in the land–atmosphere coupling system. It is replenished by precipitation and transported back to the atmosphere through land surface evaporation and vegetation transpiration. Soil moisture is, therefore, influenced by both precipitation and evapotranspiration, with spatial heterogeneities and seasonal variations across different ecological zones. However, the effects of precipitation volume, frequency, and evapotranspiration on soil moisture at different temporal scales still remain poorly understood. Negative correlations between soil moisture and precipitation have been observed in different ecosystems of the Northern Hemisphere. In this study, the response of soil moisture to precipitation from 2000 to 2019 was investigated using reanalysis data to determine the factors driving the negative correlations. The joint distributions of precipitation and soil moisture were analyzed at monthly and annual scales, using soil moisture and precipitation data from ERA5-Land and Global Precipitation Climatology Project, respectively. Nonlinear negative dependencies of soil moisture to precipitation were revealed. Based on Ridge regression models and Bayesian generalized non-linear multivariate multilevel models, these negative dependencies were shown to be most prominent in temperate grasslands, savannas, shrublands, deserts, xeric shrublands, and tundra regions and driven by the land surface temperature and by the air temperature–gross primary production relationship at the monthly scale. Additionally, the negative dependence was attributed to soil property changes induced by freeze–thaw processes, precipitation seasonality, and temperature fluctuations, which cause asynchronous variations between soil moisture and precipitation at the seasonal scale. At the annual scale, the negative dependence was linked to long-term shifts in global precipitation and temperature patterns, which affect vegetation structure and surface characteristics, thereby reducing soil water capacity. These findings enhance the understanding of land–atmosphere interactions providing a valuable basis for future research on drought, hydrometeorology, and ecological conservation.

Keywords: climate change, precipitation, soil moisture, ecoregions

https://doi.org/10.5194/egusphere-2025-762
Preprint. Discussion started: 7 March 2025
© Author(s) 2025. CC BY 4.0 License.

1. Introduction

Soil moisture is a critical source of water for vegetation growth, replenished by precipitation and groundwater, and returned to the atmosphere through evapotranspiration. It plays a key role in weather conditions, vegetation dynamics, and groundwater storage (Li et al. 2022; Qiao et al. 2023; Vereecken et al. 2008; Zhou et al. 2021), with significant implications for the global climate. Surface soil moisture regulates the distribution of available energy at the land surface and exchanges energy with the near-surface atmosphere through sensible and latent heat fluxes, thereby controlling the surface energy balance (Haghighi et al. 2018; McColl et al. 2017). In contrast, deep soil moisture is more directly influenced by vegetation growth, particularly by the development of plant roots, which play a crucial role in the vertical infiltration of precipitation into deeper soil layers (Szutu and Papuga 2019; Xiao et al. 2024; Xue and Wu 2024).

Precipitation variability, which refers to the amplitude of precipitation fluctuations over different times, influences soil moisture and thereby land surface coupling (Koster et al. 2009; Taylor et al. 2012). Precipitation patterns are reported to have undergone significant changes in recent decades (Lv et al. 2023; Mao et al. 2022; Wu et al. 2021), mainly manifested as anthropogenic amplification of precipitation variability (Zhang et al. 2024). The increase in the frequency of extreme precipitation events (Myhre et al. 2019; Wang et al. 2022) and decrease in the frequency of smaller precipitation events (Ma et al. 2015) amplify soil moisture fluctuations and prolong the moisture stress periods between consecutive precipitation events (Knapp et al. 2008). This can directly affect vegetation growth and soil moisture responses (Feldman et al. 2024; He et al. 2023), particularly through changes in the duration and intensity of soil evaporation and plant transpiration (Gu et al. 2021; Wullschleger and Hanson 2006). Soil moisture has been shown to be negatively correlated with precipitation in certain regions, based on Pearson correlation analyses (Cook et al. 2006; Yang et al. 2018). The changes in soil moisture at different depths also show notable discrepancies (Shen et al. 2016; Zhu et al. 2014). Surface soil moisture has been shown to respond to precipitation

https://doi.org/10.5194/egusphere-2025-762
Preprint. Discussion started: 7 March 2025
© Author(s) 2025. CC BY 4.0 License.

approximately a month earlier than deeper soil moisture, with a more pronounced positive correlation between precipitation and soil moisture occurring at depths greater than 50 cm (Zhang et al. 2020).

Most current analyses of the relationship between soil moisture and precipitation assume a linear relationship. In reality, the response of soil moisture to precipitation is extremely complex and often nonlinear (Drager et al. 2022). The nonlinear dependence of soil moisture to precipitation is currently not well understood. Moreover, the factors driving this negative dependence between soil moisture and precipitation remain poorly understood due to the complicated land atmosphere coupling processes, particularly in the Northern Hemisphere where different types of vegetation coverage are present. Among the methods used to explore nonlinear relationships, the copula function is one of the most widely applied approaches for modeling the joint distributions of precipitation and soil moisture (Cammalleri et al. 2024). The copula is a stochastic model that can reveal nonlinear and asymmetric dependence structures, which are difficult to capture using traditional linear methods. It provides a flexible framework for modeling joint distributions of multiple variables, allowing for a more precise understanding of the evolving dependence of soil moisture on precipitation than that offered by traditional linear regression and correlation methods.

In terms of the water cycle, soil moisture is replenished by precipitation and groundwater, while also being absorbed by plant roots and lost through evapotranspiration. Therefore, the change of soil moisture is actually simultaneously influenced by precipitation volume, frequency, and evapotranspiration. However, the response of soil moisture to precipitation and evapotranspiration varies across different time scales. The long-term effects of changes in evapotranspiration and precipitation on soil moisture are further shaped by seasonal transitions, with significant differences observed at different soil depths (Szutu and Papuga 2019). These differences are influenced by factors such as soil freeze–thaw processes and vegetation community structure. Therefore, the relative contributions of evapotranspiration, precipitation volume, and frequency to soil moisture changes should be quantified at different time

https://doi.org/10.5194/egusphere-2025-762
Preprint. Discussion started: 7 March 2025
© Author(s) 2025. CC BY 4.0 License.

scales.

Although previous studies have identified the mechanisms of soil moisture variation across different time scales (Shen et al. 2018; Vidana Gamage et al. 2020), large-scale regional patterns of soil moisture response to precipitation frequency remain poorly explored, especially in the context of climate change. In particular, the dependence of soil moisture to precipitation and its interactions with evapotranspiration under conditions of frequent extreme climate events require further investigation.

The aim of this study was to explore the nonlinear responses of soil moisture to precipitation at monthly and annual scales from 2000 to 2019, with a focus on the Northern Hemisphere where vegetation coverage is abundant. The joint distribution of precipitation and soil moisture was established to examine differences in soil moisture responses to precipitation and the varying influences of precipitation volume, frequency, and evapotranspiration on soil moisture at monthly and seasonal scales. The gross primary productivity (GPP), land surface temperature (LST), and near-surface air temperature (T_a) were selected as key driving factors in a Bayesian model, since the dependence between precipitation and soil moisture is influenced by factors such as vegetation growth, temperature, and soil properties. The driving factors and regional characteristics of the negative correlation observed between precipitation and soil moisture in certain regions were identified. This study enhances the understanding of complex interactions between key meteorological factors such as precipitation, evapotranspiration, and soil moisture under climate change, and provides a basis for future land–atmosphere coupling system modeling.

2. Material and Method

2.1 Material

2.1.1 Soil moisture

The soil moisture data used in this study were obtained from the fifth generation of reanalysis from the European Centre for Medium-Range Weather Forecasts (ECMWF), using atmospheric forcing to control the simulated land field variables and

© Author(s) 2025. CC BY 4.0 License.

provide the land components (ERA5-Land) (Muñoz Sabater 2019). ERA5-Land provides a consistent description of the evolution of the energy and water cycles over land, and therefore, has been widely used in various land surface applications such as flood or drought forecasting (Joaquín Muñoz-Sabater 2021). The ERA5-Land soil moisture data are available for four layers, 0 to 7, 7 to 28, 28 to 100, and 100 to 289 cm, at a 0.1° × 0.1° spatial and hourly temporal resolution from 1950 to present. The soil moisture from the first three soil layers during 2000 to 2019 were used. They were resampled to a 0.25° × 0.25° spatial resolution and averaged to daily, monthly, and yearly scales to be consistent with other variables in this study.

2.1.2 Precipitation

The Global Precipitation Climatology Project (GPCP) is a global precipitation project that integrates infrared and microwave data from multiple geostationary and polar-orbiting satellites, and corrected by many meteorological station observations (Adler et al. 2003; Huffman and Bolvin 2013). It is an important component of the Global Energy and Water Cycle Experiment in the World Climate Research Programme. A daily precipitation field with a 1° × 1° resolution since 1996 was generated by integrating the satellite products and then adjusting the daily precipitation by monthly data observed from the ground to make it consistent with the meteorological observations. Daily precipitation was resampled to a 0.25° × 0.25° spatial resolution and then used to calculate the total precipitation volume and precipitation frequency at the monthly, seasonal, and annual scale from 2000 to 2019.

2.1.3 Covariate variables

2.1.3.1 Gross primary production

The gross primary production (GPP) dataset was from the Vegetation Optical Depth Climate Archive v2, which used microwave remote sensing estimates of vegetation optical depth to estimate the GPP at the global scale for the period 1988 to 2020 (Wild et al. 2022). These GPP data were trained and evaluated against FLUXNET in-situ observations and compared with largely independent state-of-the-art GPP

https://doi.org/10.5194/egusphere-2025-762
Preprint. Discussion started: 7 March 2025
© Author(s) 2025. CC BY 4.0 License.

datasets from the Moderate Resolution Imaging Spectroradiometer (MODIS). The Vegetation Optical Depth Climate Archive v2 GPP dataset has a 0.25° × 0.25° spatial and half-monthly temporal resolution, covered from 2000 to 2019.

2.1.3.2 Near surface air temperature

The air temperature data (T_a) were obtained from the Climatic Research Unit gridded Time Series (CRU TS), which is one of the most widely used climate datasets and is produced by the National Centre for Atmospheric Sciences in the United Kingdom. CRU TS v4.07 was derived by the interpolation of monthly climate anomalies from extensive networks of weather station observations (Harris et al. 2020). It provides monthly land surface data from 1901 to 2020 at a 0.5° × 0.5° resolution worldwide. The mean temperatures at the monthly, seasonal, and annual scales during 2000 to 2019 were calculated and resampled to a 0.25° × 0.25° spatial resolution.

2.1.3.3 Land surface temperature

Land surface temperature (LST) data were accessed from the European Space Agency Climate Change Initiative (CCI), which is funded by the European Space Agency as part of the Agency's CCI Program. It aims to significantly improve current satellite LST data records to meet the challenging Global Climate Observing System requirements for climate applications and realize the full potential of long-term LST data for climate science (Hollmann et al. 2013). These data were the first global LST climate data records of over 25 years at a 0.25° × 0.25° resolution and with an expected error within 1 K. The LST dataset included ascending and descending orbit data, which were used to calculate the mean value of separate annual and monthly averages during 2000 to 2019.

2.1.3.4 Evapotranspiration

Evapotranspiration data were accessed from the Global Land Evaporation Amsterdam Model (GLEAM) v3.8a, which provides data of the different components of land evapotranspiration, including transpiration, bare-soil evaporation, interception loss, open-water evaporation, and sublimation, in addition to other related variables such as surface and root-zone soil moisture, sensible heat flux, potential evaporation,

https://doi.org/10.5194/egusphere-2025-762
Preprint. Discussion started: 7 March 2025
© Author(s) 2025. CC BY 4.0 License.

and evaporative stress conditions (Miralles et al. 2011). The monthly, seasonal, and annual averages during 2000 to 2019 were calculated based on a 0.25° × 0.25° spatial resolution.

2.1.3.5 Terrestrial ecoregions

Data on terrestrial ecoregions around the globe were accessed from the Conservation Biology Institute (Olson et al. 2001). These ecoregions are relatively large units of land containing distinct assemblages of natural communities and species, with boundaries that approximate the original extent of natural communities prior to major land-use changes. The delineations were completed based on hundreds of previous biogeographical studies and were refined and synthesized using existing information in regional workshops over the course of 10 years to assemble the global dataset (Olson et al., 2001). An ecological layer file encompassing 16 major categories was downloaded.

All of the T_a, LST, GPP, soil moisture, and precipitation datasets were masked by these 16 terrestrial ecoregions (Fig. 1) in a 0.25° grid, and monthly, seasonal, or annual mean values in the regions were calculated separately.

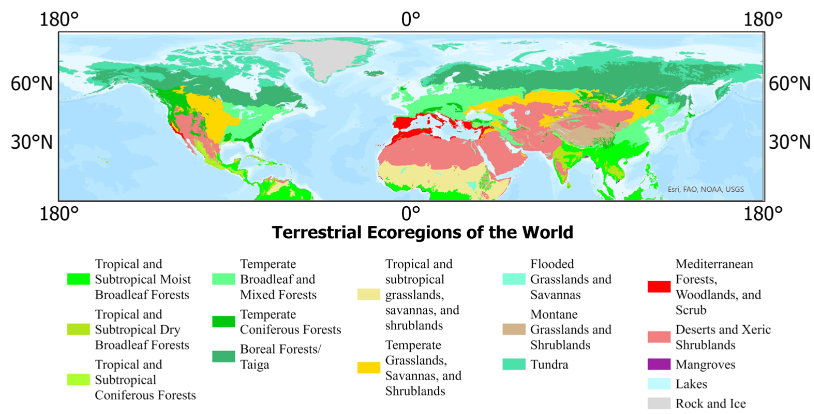

Fig. 1 The 16 Terrestrial Ecoregions of the Northern Hemisphere.

https://doi.org/10.5194/egusphere-2025-762
Preprint. Discussion started: 7 March 2025
© Author(s) 2025. CC BY 4.0 License.

2.2 Method

2.2.1 Joint distribution

In this study, the joint distribution between precipitation and soil moisture from depths of 0 to 7 cm, 7 to 28 cm, and 28 to 100 cm, using the copula function at both the monthly and annual scales was established. A copula function links multivariate distribution functions with their one-dimensional marginal distributions, and is used for the examination of dependencies between multiple variables. It captures nonlinear dependence structures through joint and marginal probabilities of a pair of variables in complex multivariate systems (Nelsen 2005). In this study, the copula function was used to explore the nonlinear dependence between precipitation and soil moisture (Equation 1):

$$F_{P,SM}(x,y) = C\big(F_P(x), F_{SM}(y)\big), \tag{1}$$

where $F_P(x)$ and $F_{SM}(y)$ denote the marginal distribution of precipitation and soil moisture, respectively, and C(u,v) is the copula function linking these two variables. The process for establishing the joint distribution was as follows: (1) The marginal distributions of precipitation and soil moisture were fitted using an automatic optimization function. (2) The most suitable copula function was selected based on the Akaike Information Criterion (AIC) values at the grid level, including Gaussian copula, Student's t copula, Clayton copula, and 37 other copula functions. Different copula functions may be selected for different grid cells. (3) The chosen copula function was then used to compute the corresponding Kendall's tau (τ), upper tail dependence (λ_U), and lower tail dependence (λ_L).

The statistic τ measures the correlation between two variables to determine the presence of a monotonic relationship. λ_U and λ_L represent the likelihood that, when one variable reaches extreme high or low values, the other variable also reaches extreme values. The calculations of τ, λ_U, and λ_L are based on the dependence parameters of the joint distribution of precipitation and soil moisture, and depends on the selected copula function using the AIC method. Taking the Tawn copula function as an example, the

https://doi.org/10.5194/egusphere-2025-762
Preprint. Discussion started: 7 March 2025
© Author(s) 2025. CC BY 4.0 License.

calculation of τ, λ_U, and λ_L are based on the following equations.

$$\tau = 1 - \frac{2\delta}{\theta+1} + \frac{2\delta^2}{2\theta+1}, \quad (2)$$

$$\lambda_U = (1-\delta) \cdot (2-2^{1/\theta}), \quad (3)$$

and

$$\lambda_L = \delta \cdot (2-2^{1/\theta}), \quad (4)$$

where θ is the dependence parameter of the Tawn copula, and δ represents the asymmetry parameter. For some copula functions, such as Clayton copula, the Kendall's τ values get the priority over the upper and lower tail dependencies in the estimation process. All the calculations were performed using R v4.3.3 with the VineCopula and copula packages, for which detailed calculation methods for τ, λ_U, and λ_L for all copulas are provided.

2.2.2 Ridge regression

Ridge regression is designed to address collinear data, although it is a biased estimation method. It is an improved least squares estimation used to generate more reliable regression coefficients at the cost of unbiasedness. Ridge regression outperforms the traditional least squares method when fitting ill-conditioned data (McDonald 2009). Due to the large uncertainty in precipitation and soil moisture data, ridge regression models were applied for three soil layers, and for both monthly and seasonal scales. Spring was defined as from March to May, summer from June to August, autumn from September to November, and winter from December to February of the following year. Precipitation frequency, volume, and evapotranspiration were treated as predictor variables, with T_a as a control variable and soil moisture as the response variable.

To clearly differentiate the influence of variables, the regression coefficients for precipitation volume, frequency, and evapotranspiration were normalized using Equation (5) and then assigned to the three primary colors. This approach resulted in a gridded ternary phase diagram.

$$W_i = 1 - \frac{v_i}{\sum_{i=1}^{3} v_i}, \quad (5)$$

https://doi.org/10.5194/egusphere-2025-762
Preprint. Discussion started: 7 March 2025
© Author(s) 2025. CC BY 4.0 License.

where $v_i(v_1, v_2, v_3)$ represent precipitation frequency, precipitation volume, and evapotranspiration (ET), respectively, and W_i refers to the adjusted weight of v_i.

2.2.3 Bayesian generalized non-linear multivariate multilevel models

The Bayesian generalized non-linear multivariate multilevel model integrates Bayesian inference, generalized linear models, non-linear modeling, multivariate analysis, and hierarchical structures, making it well-suited for complex hierarchical data. It can effectively capture non-linear dependencies among multiple response variables (Browne and Draper 2006; Bürkner 2017). The model parameters are treated as random variables with prior distributions under the Bayesian framework. Posterior distributions of the parameters are obtained by combining the likelihood function and prior distributions. The Markov Chain Monte Carlo (MCMC) algorithm is then used to resample from the posterior distribution and estimate the posterior means of the parameters to represent the optimal results. Given the hierarchical and multivariate nature of the data, a multilevel structure and multivariate analysis was introduced to model the mixed effects of variables and to capture the relationships among multiple related response variables. Random effects were also incorporated to account for heterogeneity among individuals and reflect the varying effects of univariate or multivariate mixtures on the response variables, thereby improving the accuracy of estimates.

Since the impact approaches of GPP, LST, and T_a on precipitation (P) and soil moisture (SM) are often unknown, the Gaussian distribution was specified as the prior distribution for these variables in the Bayesian model. To investigate how GPP, LST, and T_a influence the precipitation–soil moisture coupling relationship, both precipitation and soil moisture were treated as response variables. Bayesian non-linear multivariate multilevel models were developed at both the monthly and seasonal scales, with independent models for 16 ecological zones (Equation 6):

$$\text{Posterior estimates} = \text{bf}(\text{P} \sim \text{T}_\text{a} + \text{GPP} + \text{LST} + \text{T}_\text{a}\text{:GPP} + \text{T}_\text{a}\text{:LST} + \text{GPP:LST} + \text{T}_\text{a}\text{:GPP:LST}) + \text{bf}(\text{SM} \sim \text{T}_\text{a} + \text{GPP} + \text{LST} + \text{T}_\text{a}\text{:GPP} + \text{T}_\text{a}\text{:LST} + \text{GPP:LST} + \text{T}_\text{a}\text{:GPP:LST}), \quad (6)$$

https://doi.org/10.5194/egusphere-2025-762
Preprint. Discussion started: 7 March 2025
© Author(s) 2025. CC BY 4.0 License.

where the colon represents multivariate mixed effects of different variables; bf stands for Bayesian formula, used to specify each part of the model for P and SM separately; and the "+" combines P and SM into a multivariate model. The model was implemented in R 4.3.3 using the brms package, which performs diagnostic checks on the sampling results using indicators such as the Gelman–Rubin diagnostic (Rhat statistic) and the effective sample size (ESS). To ensure stability and convergence, four MCMC chains were used for iterative sampling, with each chain running 4,000 iterations, including 2,000 warm-up iterations. A maximum tree depth of 10 was set. Estimate values of all ecoregions were classified into different clusters using the K-means method in R 4.3.3.

3. Results

3.1 Estimation from the copula function

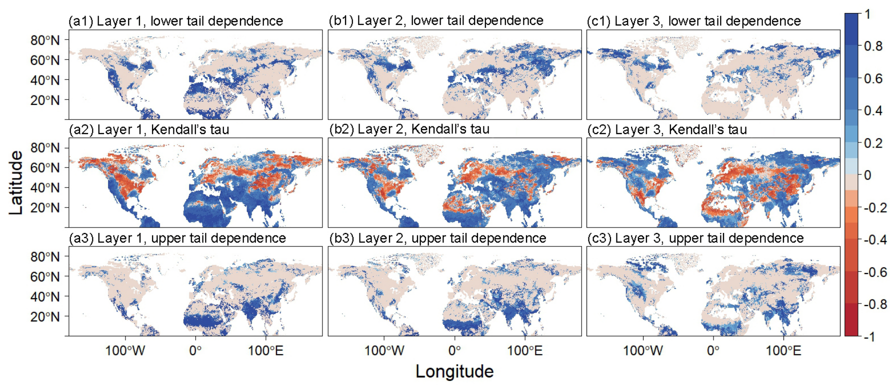

Fig. 2 Spatial distribution of Kendall's tau (τ), the upper tail dependence (λ_U), and the lower tail dependence (λ_L) on the 0.25° × 0.25° grids between monthly precipitation volume and soil moisture during 2000 to 2019. The three columns are for the soil moisture from depths of 0 to 7 cm, 7 to 28 cm, and 28 to 100 cm, respectively.

The copula analysis of monthly average soil moisture and total monthly precipitation volume revealed a clear negative dependence at all three soil depths (a2, b2, and c2; Fig. 2). The percentages of grid cells exhibiting negative dependence at these depths were 29.3%, 25.3%, and 30.9%, respectively. Regions with negative

https://doi.org/10.5194/egusphere-2025-762
Preprint. Discussion started: 7 March 2025
© Author(s) 2025. CC BY 4.0 License.

dependence were primarily located in the eastern United States, central and northern Russia, northern Asia, and the Sahara Desert. The extent of the negative dependence expanded significantly with an increase in soil depth in the Sahara, and covered much of northern Africa. In North America and northern Asia, the negative dependence was most prominent in the ecological zones of temperate grasslands, savannas, and shrublands, with additional occurrences in the deserts and xeric shrublands and tundra regions.

Regions exhibiting high λ_L values were primarily located in the northern and western United States, eastern Russia, the temperate coniferous forests of Mongolia, and the Mediterranean forests, woodlands, and scrublands of Africa (a1, b1, c1; Fig. 2). The extent of areas showing dependence decreased as soil depth increased. Similarly, λ_U exhibited a clear reduction in spatial extent with increasing soil depth, with the majority of these regions located in the southern Sahara Desert, India, southern and eastern China, and small parts of northern Russia. However, no clear correspondence between these regions and specific ecological zones was observed (a3, b3, c3; Fig. 2).

From the annual scale copula results (Fig. 3), precipitation and soil moisture generally exhibited positive dependencies across the entire soil profile. However, negative dependencies were observed in regions such as the southern Sahara Desert, Mongolia, and the Elizabeth Islands, reaching 3.0%, 4.0%, and 8.6%, respectively (a2, b2, c2; Fig. 3). The negative dependencies in these areas expanded outward, primarily concentrated in the montane grasslands and shrublands region. Both the λ_L and the λ_U displayed scattered, patchy distributions, with average values for each soil layer ranging from 0.4 to 0.6.

https://doi.org/10.5194/egusphere-2025-762
Preprint. Discussion started: 7 March 2025
© Author(s) 2025. CC BY 4.0 License.

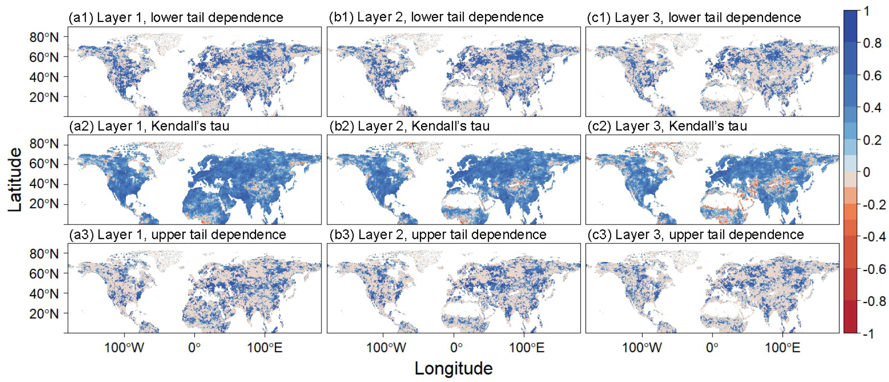

Fig. 3 Spatial distributions of the τ, λ_U, and λ_L on the 0.25° × 0.25° grids between annual precipitation volume and soil moisture during 2000 to 2019. The three columns are for the soil moisture from depths of 0 to 7 cm, 7 to 28 cm, and 28 to 100 cm, respectively.

3.2 Control of soil moisture by precipitation and evapotranspiration

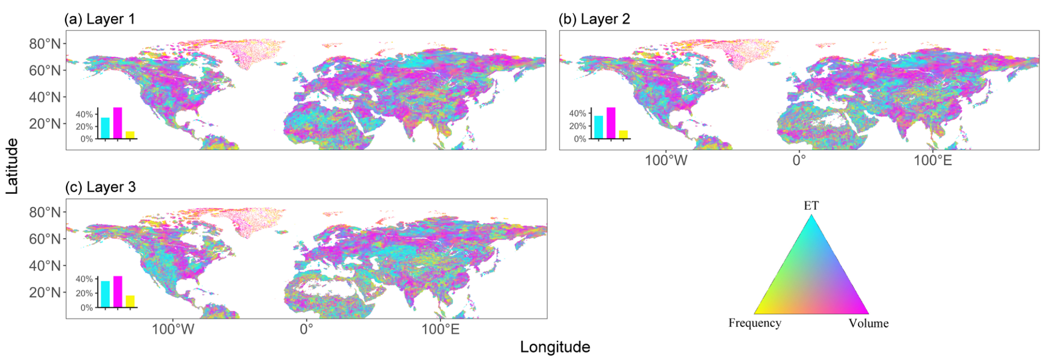

Fig. 4 Ternary map of factors controlling soil moisture, monthly, for the period 2000 to 2019. The bottom-left histogram in the subgraph represents the proportion of grid cells where one variable exerts strong univariate control (with a regression coefficient greater than 75% of the total sum of the three variables), suggesting that soil moisture was predominantly controlled by that specific variable.

On the monthly scale, precipitation exerted the strongest control over soil moisture (Fig. 4), with regions most influenced by precipitation accounting for more than 40% of the variation. These areas were primarily located in the boreal forest/taiga, temperate

https://doi.org/10.5194/egusphere-2025-762
Preprint. Discussion started: 7 March 2025
© Author(s) 2025. CC BY 4.0 License.

grasslands, savannas, shrublands, and the eastern part of North America. In contrast, regions where evapotranspiration predominated were found in Alaska–Northwest Canada, the western United States, the Sahara Desert, and the Middle East. High-latitude regions, especially northern Canada, were primarily influenced by precipitation frequency. Areas where precipitation volume, frequency, and evapotranspiration had similar levels of control were mainly found in Eastern Europe and Russia.

The results from ridge regression revealed more distinct patterns at the seasonal scale compared to the monthly scale (Fig. 5). Soil moisture in spring and summer was mainly controlled by evapotranspiration, which influenced over 40% of grid cells, particularly in the middle soil layers, where it dominated nearly 80%. In contrast, precipitation volume had a greater influence during autumn and winter, particularly in the continental United States, southern Sahara Desert, coastal India, and eastern China. Additionally, as soil depth increased, the influence of evapotranspiration and precipitation frequency gradually intensified. However, in summer, as soil depth increased, the area primarily controlled by precipitation volume expanded (indicated by an increase in the intensity of magenta color in the figures) especially in the eastern United States, Europe, and South Asia. These regions remained strongly influenced by precipitation volume even as evapotranspiration control increased with increasing soil depth during autumn. Northern Russia, Canada, Greenland, and northern Alaska were notably influenced by both precipitation frequency and precipitation volume, with this effect being more pronounced during the non-growing season. In winter, the area controlled by precipitation frequency was larger than that in spring.

https://doi.org/10.5194/egusphere-2025-762
Preprint. Discussion started: 7 March 2025
© Author(s) 2025. CC BY 4.0 License.

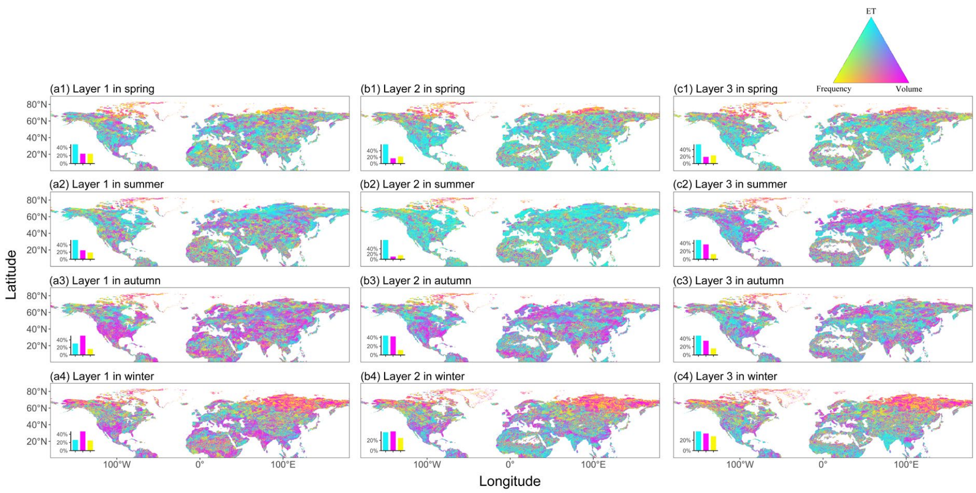

Fig. 5 Ternary map of factors controlling soil moisture, annually, for the period 2000 to 2019. The bottom-left histogram in the subgraph represents the proportion of the grid cells where one variable exerts strong univariate control (with a regression coefficient greater than 75% of the total sum of the three variables), suggesting that soil moisture was predominantly controlled by that specific variable.

3.3 Drivers of negative dependencies between soil moisture and precipitation

For each model in this study, four MCMC chains were used for iterative sampling. The sampling results demonstrated that the chains for both the monthly and annual scales were well-distributed in the parameter space, with no noticeable trends or drifts, indicating convergence to the target posterior distribution. The convergence was considered satisfactory, with all models yielding a Rhat value below 1.05 (Fig. S1, S2).

https://doi.org/10.5194/egusphere-2025-762
Preprint. Discussion started: 7 March 2025
© Author(s) 2025. CC BY 4.0 License.

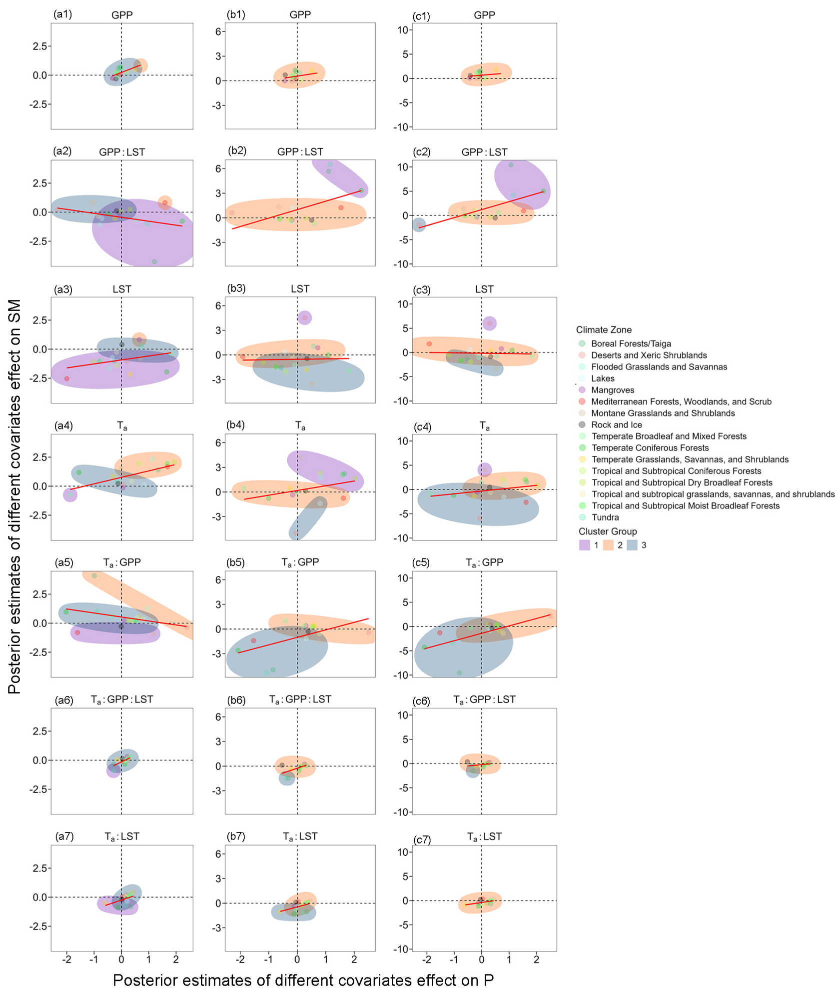

Fig. 6 Posterior estimates of the covariate variables of the Bayesian generalized non-linear multivariate multilevel model, built using monthly data. The columns represent soil depths of 0 to 7 cm, 7 to 28 cm, and 28 to 100 cm. Red lines indicate linear regressions of precipitation and soil moisture across all ecoregions, with cluster groups represented by three circles.

The fitted values of multiple drivers for both precipitation and soil moisture were calculated. When precipitation and soil moisture were either positive or negative simultaneously (quadrants I and III), the driver promoted a positive dependence between the two variables. Conversely, when they were in quadrants II and IV, the

https://doi.org/10.5194/egusphere-2025-762
Preprint. Discussion started: 7 March 2025
© Author(s) 2025. CC BY 4.0 License.

driver induced a negative dependence. A comparison of these results with those in Section 3.1 shows that the negative dependence observed at the monthly scale in the temperate grasslands, savannas, and shrublands was driven by LST and T_a:GPP across all three soil layers, particularly in quadrant IV, where precipitation increased while soil moisture decreased. Other factors, however, drove a positive dependence (Fig. 6).

The negative dependence between precipitation and soil moisture in the surface layer across the Northern Hemisphere was primarily driven by the interactions between GPP:LST and T_a:GPP. The regression trend line intersected quadrants II and IV. Ecological zones affected by GPP:LST included temperate coniferous forests, boreal forests, tundra, and temperate broadleaf mixed forests. The negative relationship driven by GPP:LST was predominantly concentrated in quadrant IV, where increased precipitation lead to decreased soil moisture in the boreal forest, tundra, temperate coniferous forest, and temperate broadleaf mixed forest, while GPP:LST driven decreased precipitation and increased soil moisture in deserts and xeric shrublands. In contrast, GPP:LST also drove a negative dependence in the middle soil layer and a positive dependence in the deep soil layers of deserts and xeric shrublands. The negative dependence driven by T_a:GPP was mainly found in quadrant II, with distributions in deserts and xeric shrublands, boreal forests, montane grasslands and shrublands, temperate broadleaf mixed forests, and tundra. LST also influenced temperate coniferous forests, temperate broadleaf mixed forests, and deserts and xeric shrublands, all of which were located in quadrant IV.

In contrast, for the middle soil layer, all regression slopes of the variables were positive. GPP, T_a:GPP:LST, and T_a:LST had minimal impact across all ecological zones, with estimated values near the origin and only two distinct clustering results. The first cluster was located in quadrant I, while the second cluster exhibited some negative dependence, affecting a small portion of forests and shrublands. This cluster was relatively flat, particularly with LST and T_a crossing the x-axis, suggesting that changes in precipitation were driven by LST and T_a, while soil moisture remained constant.

The negative dependence between precipitation and soil moisture in the deep soil

https://doi.org/10.5194/egusphere-2025-762
Preprint. Discussion started: 7 March 2025
© Author(s) 2025. CC BY 4.0 License.

layers was partly driven by the second and third clusters. GPP:LST drove a reduction in precipitation and an increase in soil moisture in tropical and subtropical grasslands, savannas, shrublands, and tropical and subtropical coniferous forests. T_a and T_a:GPP drove an increase in precipitation and a decrease in soil moisture in Mediterranean forests, woodlands, and scrub, as well as in temperate grasslands, savannas, and shrublands. The mixed effects of T_a:GPP:LST and T_a:LST had minimal impact across all ecological zones, with all estimates concentrated near the origin and only two clusters observed. The second cluster was primarily located in quadrant I, where both precipitation and soil moisture increased, leading to a positive dependence between them. The negative dependence observed in the third cluster, distributed across quadrants II and IV, showed decreased precipitation and increased soil moisture in quadrant II, and increased precipitation and decreased soil moisture in quadrant IV. Most of the affected ecoregions were forest types.

https://doi.org/10.5194/egusphere-2025-762
Preprint. Discussion started: 7 March 2025
© Author(s) 2025. CC BY 4.0 License.

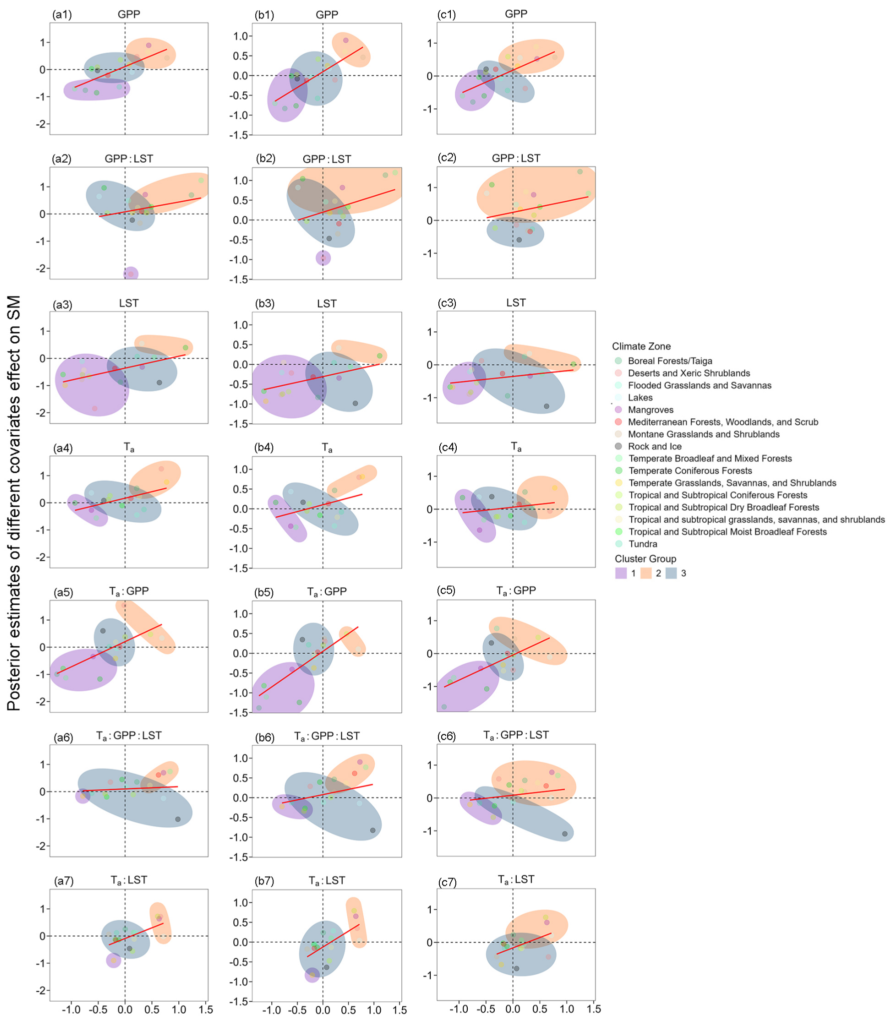

Fig. 7 Posterior estimates of the covariate variables of the Bayesian generalized non-linear multivariate multilevel model, built using annual data. The columns represent soil depths of 0 to 7 cm, 7 to 28 cm, and 28 to 100 cm. Red lines indicate linear regression of precipitation and soil moisture across all ecoregions, with cluster groups represented by three circles.

Interannual negative dependence was primarily observed in the montane grasslands and shrublands region, where GPP:LST drove this pattern across all three soil layers. All other variables lead to positive dependence (Fig. 7). The long-term trend

https://doi.org/10.5194/egusphere-2025-762
Preprint. Discussion started: 7 March 2025
© Author(s) 2025. CC BY 4.0 License.

in the annual-scale Bayesian model revealed strong patterns, with the most significant difference compared to the monthly scale being the influence of T_a:GPP:LST and T_a:LST, where different ecological zones exhibited substantial variation. The second cluster across all soil layers was consistently distributed in quadrant I, while the boundaries of the first cluster were located in quadrant III, far from the origin. The third cluster spanned quadrants II and IV, with its origin in quadrant IV, suggesting that nearly all variables drove an increase in precipitation and a decrease in soil moisture in the ecological zones of the third cluster. Among the multiple variables, T_a drove the most negative dependence, with the greatest differences observed between ecological zones.

In the surface layer, LST alone drove the negative dependence in the mangrove, rock, and ice regions, which are characterized by extremely wet soils. T_a drove the negative dependence, resulting from decreased precipitation and increased soil moisture, in tropical and subtropical coniferous forests, lakes, and rock and ice regions. Additionally, T_a drove the negative dependence in temperate broadleaf and mixed forests and tundra regions, where precipitation increased with a decrease in soil moisture.

In the middle soil layers, the negative dependence driven by T was evenly distributed across quadrants II and IV. In temperate forests, arid shrublands, and flooded grasslands and savannas, the negative dependence was characterized by increased precipitation and decreased soil moisture. In contrast, in tropical and subtropical coniferous forests and temperate coniferous forests, the negative dependence was marked by decreased precipitation and increased soil moisture. The negative dependence driven by T_a:GPP was entirely due to reduced precipitation and increased soil moisture in tropical and subtropical moist broadleaf forests. The negative dependence driven by T_a:LST was fully distributed in quadrant IV, where it was characterized by increased precipitation and decreased soil moisture. This pattern was observed in regions such as the montane grasslands and shrublands; tropical and subtropical coniferous forests; tropical and subtropical grasslands, savannas, and shrublands; and rock and ice regions.

https://doi.org/10.5194/egusphere-2025-762
Preprint. Discussion started: 7 March 2025
© Author(s) 2025. CC BY 4.0 License.

In the deep soil layers, the dependencies across different ecological zones were more dispersed. GPP, GPP:LST, and T_a:GPP exhibited a strong positive dependence trend, with slopes close to 1. In contrast, the positive dependence driven by T_a and T_a:GPP:LST had smaller slopes, nearly parallel to the x-axis, suggesting an increase in precipitation as soil moisture remained constant. The strongest drivers of negative dependence in the deep layers were GPP:LST and T_a. The negative dependence driven by GPP:LST was found in the ecological zones of quadrant IV, including rock and ice regions, Mediterranean forests, woodlands, and scrub, as well as tundra and temperate coniferous forests in quadrant II. The negative dependence driven by T_a was observed in rock and ice regions, lakes, and temperate coniferous forests in quadrant II, and flooded grasslands and savannas in quadrant IV.

4. Discussion

4.1 Characteristics of negative dependence areas

In this study, joint distributions of precipitation and soil moisture were constructed using Kendall's τ to characterize the nonlinear relationship between them. The analysis revealed a negative dependence between precipitation and soil moisture at both the monthly and annual scales from 2000 to 2019. The τ value at the monthly scale was higher than that at the annual scale, with a larger area exhibiting a negative dependence. Therefore, seasonal variations likely contributed to the negative dependence at the monthly scale, while long-term trends, particularly the Arctic amplification effect associated with global climate change, drove the negative dependence at the annual scale.

Regions exhibiting negative dependence, such as deserts and xeric shrublands, temperate grasslands, savannas, shrublands, and tundra, are all arid or semi-arid and characterized by shrub-dominated communities with little or no tree growth (Olson and Dinerstein 1998). Deserts and xeric shrublands show significant annual precipitation variability across the region. Except for the peripheral areas, annual precipitation typically does not exceed 250 mm, and evaporation exceeds precipitation (Lockwood et al. 2006). The tundra, a treeless desert found in high-latitude Arctic regions (also known as polar desert), is primarily distributed in Alaska, Canada, Russia, Greenland, Iceland, and Scandinavia, as well as the sub-Antarctic islands (Olson and Dinerstein 1998). Vegetation in this region is sparse, with dry winters and extremely low temperatures (Xue et al. 2021). The average annual precipitation is approximately 350 mm, and the dominant vegetation includes sedges, heaths, and dwarf shrubs (Olson and Dinerstein 1998).

Temperate grasslands, savannas, and shrublands differ from other ecosystems in several ways. In North America, this ecosystem is known as prairie, in South America as pampas, in Southern Africa as veld, and in Asia as steppe. These ecosystems differ significantly from tropical grasslands, particularly in their annual temperature regime and the types of species present. Typically, these regions lack trees, except for riparian or gallery forests along streams and rivers. However, some areas support savanna conditions, characterized by scattered individuals or clusters of trees (Olson and Dinerstein 1998). A defining feature of temperate grasslands is that the dominant vegetation consists of grasses, with little to no trees or large shrubs. These regions experience a large temperature difference between summer and winter, moderate precipitation, and fertile soils. On the monthly scale, regions with a negative dependence between precipitation and soil moisture are generally arid or semi-arid and lack tree growth (Olson and Dinerstein 1998). Additionally, studies have shown that soil moisture influences precipitation primarily by increasing it in arid regions (Donat et al. 2017).

The clear dependencies between precipitation and soil moisture in Mediterranean forests, woodlands, and scrub were driven by the highly seasonal nature of meteorological drought in the Mediterranean climate zone, typically occurring in the summer. During the winter, when precipitation was insufficient, soil moisture was rapidly depleted, leading to soil drought in the summer and consequently high levels of soil temperature–drought (high λ_L). However, extreme precipitation did not necessarily result in a sharp increase in soil moisture, and this was influenced by factors such as

https://doi.org/10.5194/egusphere-2025-762
Preprint. Discussion started: 7 March 2025
© Author(s) 2025. CC BY 4.0 License.

vegetation community structure, soil texture, and geographical conditions, which account for the lack of distinct ecological zone differences in λ_U.

4.2 Main control factors in negatively dependent regions

The seasonal scale exhibited a clear pattern: The growing season was primarily controlled by evapotranspiration, while the non-growing season was driven by precipitation. During spring and summer, adequate precipitation and higher temperatures fostered vegetation growth. The high temperature and precipitation during these periods accelerated evapotranspiration. Soil moisture in the surface layers of the Northern Hemisphere was therefore controlled by evapotranspiration, while the middle soil layers were influenced by plant transpiration. In deep soil layers (28–100 cm in ERA5-Land), root density decreases (Stocker et al. 2023), and only certain forest species and drought-adapted shrubs with extensive root systems contribute to transpiration. Consequently, precipitation percolates into the deep soil layers, where it is retained. In high-latitude regions, characterized by temperature-limited ecosystems with low annual precipitation, conifer species (e.g., *Abies*, *Picea*, *Larix*, and *Pinus*) dominate, with a limited presence of deciduous trees (Walker et al. 2016). In the boreal forests of North America, Canada, and Siberia, winters are long and harsh, while summers are short and cool. The low temperatures constrain evapotranspiration and plant transpiration rates. Despite the presence of some deciduous forests, soil moisture during the non-growing season is primarily controlled by precipitation rather than by evapotranspiration due to the extremely low temperatures. Similarly, precipitation dominates soil moisture regulation in temperate grasslands, savannas, and shrublands, which experience semi-arid to humid climates. These regions receive annual precipitation ranging from 150 to 1200 mm and average temperatures between 0 and 25°C (Sala et al. 2001). The soils in these grasslands are generally highly permeable with moderate water-holding capacity, allowing precipitation to infiltrate easily and replenish deep soil moisture. Grassland root systems both suppress surface evaporation and promote transpiration. During the rainy season, most water percolates into the soil, where it is stored in deep layers, creating a reservoir effect (Scholes and Walker 1993).

https://doi.org/10.5194/egusphere-2025-762
Preprint. Discussion started: 7 March 2025
© Author(s) 2025. CC BY 4.0 License.

This stored moisture becomes the primary water source for vegetation during the dry season. As the dry season progresses, soil moisture is gradually depleted until it is completely exhausted. Thus, the reduction in soil moisture during the growing season is mainly due to rapid consumption through evapotranspiration, while in the non-growing season, it is primarily caused by insufficient precipitation replenishment.

Autumn and winter mark the dry season for much of the Northern Hemisphere, when evapotranspiration rates decrease. Studies have shown that during the freezing seasons, larger snow depths help maintain soil temperature and mitigate the impact of frost on the soil. For certain narrow frozen soils, sufficiently thick snow may also allow more meltwater to infiltrate into the soil (Jafarov et al. 2018). As a result, high-latitude regions are more strongly influenced by precipitation frequency and volume during autumn and winter.

4.3 Mechanism of negative dependence between precipitation and soil moisture

The negative dependence between precipitation and soil moisture in the temperate grasslands, savannas, and shrublands was primarily driven by LST and T_a:GPP. These regions, characterized by a semi-arid climate, experienced joint control by precipitation and evapotranspiration in both surface and deep soil layers. During the growing season, high evaporation and plant transpiration rates rapidly depleted soil moisture in the surface layer, with the combined effects of higher LST and T_a:GPP driving the negative dependence. This negative relationship was also observed in deserts, xeric shrublands, montane grasslands, shrublands, and tundra. The climate of these ecoregions are typically dry, with high evapotranspiration and low precipitation, limiting the accumulation and retention of soil moisture. In high-temperature environments, increased evapotranspiration rates and VPD exacerbate soil moisture depletion, even when precipitation increases. These regions generally have a low GPP, and the effective use of precipitation by vegetation is limited (Xue and Wu 2023), intensifying the negative dependence between precipitation and soil moisture. The montane grasslands

https://doi.org/10.5194/egusphere-2025-762
Preprint. Discussion started: 7 March 2025
© Author(s) 2025. CC BY 4.0 License.

and shrublands, located at higher altitudes, experience more extreme temperature fluctuations (Olson and Dinerstein 1998). In mountainous regions, the likelihood of warming is higher than in lowland areas (Pepin et al. 2022), which leads to a rapid increase in evapotranspiration rates. Although GPP may increase with higher temperatures, the vegetation in these areas typically grows slowly and is characterized by shallow root systems (Stocker et al. 2023), limiting its ability to use additional precipitation and resulting in a reduction in surface soil moisture.

Soil moisture reduction in the 7-to-28-cm depth due to evapotranspiration was driven by several factors, the primary one being the absorption of soil water by plant roots under conditions of high LST and GPP. Additionally, the arid surface soil induced upward movement of soil water from the middle layer due to the osmotic and matric potential, further contributing to moisture depletion. The water compensation mechanism of plant roots can also lead to reduced water uptake in the surface layer during dry conditions and an increased uptake in the wetter layers (Yadav Brijesh et al. 2009). Furthermore, summer precipitation is often unstable, and heavy rainfall fails to rapidly penetrate the deep soil layers. As a result, at this depth, soil moisture reduction is predominantly driven by high land surface temperature and evapotranspiration. Intense evapotranspiration during the growing season transports moisture to the atmosphere, increasing vapor pressure and promoting precipitation. However, even with increased rainfall, the water demands of vegetation and evapotranspiration are insufficiently met. Additionally, high temperatures can lead to surface soil sealing, preventing rainfall from effectively entering the root zone.

During the non-growing season, low temperatures reduce evapotranspiration rates, and soil moisture is primarily controlled by precipitation volume and frequency. In cold conditions, precipitation often falls as snow, which accumulates on the surface. A low LST can cause soil freezing, and the presence of surface litter may further insulate the soil, preventing timely moisture replenishment. Although evapotranspiration is reduced, some deep-rooted plants may continue to absorb water to a limited extent. Additionally, during precipitation intervals, soil moisture may gradually decrease due to residual evapotranspiration, micro-scale runoff, or plant water consumption (Tomlinson et al. 2013), leading to a negative dependence between precipitation and soil moisture. Empirical studies have shown that in temperate grasslands, savannas, and shrublands, plants retain their leaves during the dry season to facilitate evaporative cooling and protect against temperature fluctuations (Prior et al. 1997). This strategy is also observed in regions with similar climatic conditions, such as deserts and xeric shrublands, where during dry winters, precipitation and soil freezing reduce soil moisture.

The boreal forest and tundra ecosystems, located in the circumpolar Arctic, are temperature-limited systems. Permafrost in these regions can lead to surface runoff of some precipitation, preventing effective infiltration into the soil. Additionally, canopy interception further limits soil moisture. As a result, in higher-latitude ecosystems such as the boreal forest, tundra, temperate coniferous forests, and temperate broadleaf-mixed forests, surface soil moisture tends to decrease. In these regions, an increase in LST and T_a mitigates the effects of temperature limitation, allowing precipitation to infiltrate the soil. This transforms the precipitation–soil moisture relationship in boreal forests and tundra from a negative to a positive dependence. In contrast, in temperate broadleaf and mixed forests, the negative dependence of increased precipitation and reduced soil moisture is primarily driven by high evapotranspiration. These forests experience warm, humid summers and cool, moderate winters, with ample and evenly distributed annual precipitation. The vegetation is a mix of deciduous species (e.g., *oak, maple, beech*) and coniferous species (e.g., *pine, spruce*) (Olson and Dinerstein 1998). Due to the moderate climate, species diversity in these forests is relatively high. While precipitation and soil moisture infiltration support the water cycle, the high rate of evapotranspiration can lead to rapid depletion of surface soil moisture, despite ample precipitation.

The negative dependence observed in mid-to-deep soil layers may occur when a single variable predominates, limiting the compensatory mechanisms within the ecosystem. In contrast, a positive dependence driven by mixed effects can result from

https://doi.org/10.5194/egusphere-2025-762
Preprint. Discussion started: 7 March 2025
© Author(s) 2025. CC BY 4.0 License.

a synergistic interaction between GPP and LST. For instance, an increase in GPP suggests an enhanced water-use efficiency or a deeper root growth, which allows for more effective water uptake. At the same time, an increase in LST may facilitate moisture release from the soil, providing additional water resources for plants. This synergistic effect can counterbalance or even reverse the negative effects of a single variable, leading to a positive dependence. Moreover, feedback mechanisms within the ecosystem may be strengthened when both GPP and LST interact. For example, a higher GPP indicates an increased rate of photosynthesis and a higher biomass accumulation, which help improve the soil structure by increasing the organic matter content and thereby enhancing soil water retention. In this scenario, the rise in LST may not result in significant moisture loss, as the improved soil structure can offset the increase in evapotranspiration, fostering a positive dependence. Another possibility is that when both GPP and LST act together, the ecosystem may exhibit greater resilience, enabling it to adapt to changes in soil moisture and precipitation. For example, an increased GPP could improve the plant's water-use efficiency, while the rise in LST could release more soil moisture through freeze–thaw processes in colder regions, resulting in more available water for plant uptake. This balancing mechanism helps maintain ecosystem stability, resulting in a positive dependence.

The interannual negative dependence between precipitation and soil moisture is increasingly observed under global climate change. The biomes of the montane grasslands and shrublands include the Puna and Paramo in South America, the Subalpine Heath in New Guinea and East Africa, the Steppes of the Qinghai–Tibetan Plateau, and other subalpine habitats worldwide (Olson and Dinerstein 1998). These ecoregions, located in tropical, subtropical, and temperate regions, are particularly vulnerable to the effects of climate change. High-altitude ecosystems are expected to experience more frequent warm periods and fluctuations in precipitation, with more pronounced feedbacks as they face long-term climatic stress (Lamprecht et al. 2018). Montane grasslands and shrublands are adapted to long-term cold, moist conditions and strong solar radiation, with vegetation extending to altitudes of up to 4500 to 4600 m

https://doi.org/10.5194/egusphere-2025-762
Preprint. Discussion started: 7 March 2025
© Author(s) 2025. CC BY 4.0 License.

(Olson and Dinerstein 1998). However, global climate change, particularly in the Arctic and the Qinghai–Tibetan Plateau, is driving rapid warming in permafrost regions. Field experiments have shown that higher temperatures may lead to a decrease in species abundance and an increase in GPP in high-altitude vegetation communities (Berauer et al. 2019). Studies also suggest that the standardized abundance of montane grasslands and shrubland communities is negatively correlated with soil magnesium and phosphorus content, carbohydrate metabolism, virulence, motility, and organic nitrogen and sulfur (Graham Emily et al. 2024). The increased frequency of extreme precipitation and rising LST facilitate the release of soil minerals and decrease microbial biomass (Siebielec et al. 2020). Improvements in soil nutrient status often lead to intensified competition for radiation, further reducing ecosystem stability. The decline in biodiversity directly diminishes ecosystem resilience, which in turn lowers soil water capacity. Additionally, 14.5% of global montane grasslands face a high risk of water erosion (Straffelini et al. 2024), presenting significant challenges for soil and water conservation. While the Arctic tundra is also at risk of shrubification due to warming, it remains relatively drier, with extreme precipitation far below that of the montane grasslands and shrublands. On an annual scale, montane grasslands and shrublands are primarily controlled by evapotranspiration, and the combination of this control with a decline in soil water capacity results in a clear negative dependence: As precipitation increases, soil moisture decreases, driven by the interaction between GPP and LST.

In semi-arid and arid grassland systems, brief precipitation events typically only moisten the upper clay layers, where most grass roots are concentrated (Sala and Lauenroth 1985). Well-developed clay layers can store infiltrated water, but they also prevent the deeper expansion of shrub vegetation roots (Buxbaum and Vanderbilt 2007). As GPP and LST increase, the loss of water stored in the upper clay layers through evapotranspiration is exacerbated, resulting in a negative dependence between precipitation and soil moisture. Additionally, model simulations suggest that in regions with simple topographic structures, such as arid and semi-arid grasslands and

https://doi.org/10.5194/egusphere-2025-762
Preprint. Discussion started: 7 March 2025
© Author(s) 2025. CC BY 4.0 License.

shrublands, precipitation has a significant effect on soil moisture (Koukoula et al. 2021). Dry soils are also more prone to surface runoff during precipitation events, a phenomenon known as the "dry soil advantage."

4.4 Data reliability

The CRU TS dataset used in this study is based on ground-based meteorological station observations, while the ESA CCI dataset is derived from satellite-based surface temperature measurements. The GPCP dataset combines both ground-based observations and satellite data, which are directly based on actual observational data. In contrast, the ERA5-Land dataset is generated using ERA5 as the forcing data. While ERA5 provides a comprehensive range of meteorological data and is widely used, it relies on numerical weather prediction models, which are based on principles of atmospheric physics. These models use observational data to calibrate their outputs, and using ERA5 meteorological data, uncertainties inherent in the model are introduced. Consequently, different sources of meteorological data were selected for this study.

All data were clipped according to the boundaries of Terrestrial Ecoregions, which were integrated from multiple studies by the Conservation Biology Institute. These ecoregions are based on different criteria across regions and are widely accepted, although they may be controversial in some areas. Therefore, discussing the driving factors of the negative dependence between precipitation and soil moisture in these regions may involve potential biases and uncertainties.

Given the clear seasonal variations in precipitation and evapotranspiration and the minimal interannual variability, precipitation volume, frequency, and control of evapotranspiration on soil moisture were analyzed at both the monthly and seasonal scales. The study also explored the precipitation–soil moisture dependence and its driving factors at the monthly and annual scales. While seasonal and interannual variations were observed, the seasonal scale was omitted to emphasize the seasonality of evapotranspiration. In the Bayesian models, the discussion focused on GPP, temperature, and LST as driving factors. Since temperature and soil moisture are input variables for evapotranspiration calculations, evapotranspiration was excluded from the

https://doi.org/10.5194/egusphere-2025-762
Preprint. Discussion started: 7 March 2025
© Author(s) 2025. CC BY 4.0 License.

analysis as a negative dependence driver.

In addition to the factors discussed in this study, other variables such as wind patterns and topography may also influence the negative dependence between precipitation and soil moisture. While this study provides a foundational analysis of the negative dependencies across different ecoregions, future research should explore these aspects further.

5. Conclusion

This study explored the dependence relationships between precipitation and soil moisture at depths of 0 to 7 cm, 7 to 28 cm, and 28 to 100 cm from 2000 to 2019, by examining the control effect of precipitation volume, precipitation frequency, and evapotranspiration on soil moisture. Bayesian models were used to analyze the driving factors in the dependence of soil moisture to precipitation in different ecoregions of the Northern Hemisphere. The results suggest that, at the monthly scale, precipitation volume predominantly controlled soil moisture in the Boreal forest/taiga, temperate grasslands, savannas, and shrublands, while precipitation frequency primarily controlled soil moisture in the high-latitude regions of the Northern Hemisphere. The combined influence of evapotranspiration and precipitation exhibited clear seasonal patterns. Evapotranspiration was the main driver during the growing season, while precipitation volume dominated in the non-growing season. As latitude increased, the influence of precipitation frequency on soil moisture also increased.

In regions such as temperate grasslands, savannas, shrublands, deserts, xeric shrublands, and tundra, negative dependencies between precipitation and soil moisture, driven by LST and T_a:GPP interactions, were observed. These negative dependencies were mainly attributed to the seasonality of precipitation in arid and semi-arid areas and the freeze–thaw processes in the soil, which hinder effective moisture replenishment, especially during winter when soil freezing prevents rainwater infiltration. In the intermediate and deep soil layers, negative dependencies were primarily driven by single variables, whereas positive dependencies resulted from multivariate interactions, likely due to the lack of compensatory mechanisms when a single variable dominated,

https://doi.org/10.5194/egusphere-2025-762
Preprint. Discussion started: 7 March 2025
© Author(s) 2025. CC BY 4.0 License.

or the enhancement of ecosystem feedbacks when both GPP and LST interacted. Additionally, when the ecosystem is simultaneously driven by GPP and LST, greater resilience may be exhibited.

At the annual scale, the area of negative dependence increased with soil depth, with the most pronounced negative dependencies occurring in the montane grasslands and shrublands region. In this region, negative dependencies at all three soil depths were driven by the GPP:LST interaction. The main cause of the negative dependence in the montane regions was the long-term variability in precipitation and temperature, which lead to changes in geomorphology and vegetation community structure, ultimately reducing the soil water capacity. Another potential cause of the negative dependence is the detrimental effect of increased extreme precipitation on microbial activity and ecosystem resilience in these regions.

Data availability

ERA5-Land soil moisture dataset can be accessed at https://cds.climate.copernicus.eu/datasets/reanalysis-era5-land?tab=overview (accessed on 18 Mar 2024). GPCP precipitation dataset can be accessed at https://www.ncei.noaa.gov/data/global-precipitation-climatology-project-gpcp-daily/access/ (accessed on 11 Mar 2024). The Gross primary production dataset can be accessed at https://researchdata.tuwien.ac.at/records/1k7aj-bdz35 (accessed on 23 Oct 2023). Climatic Research Unit gridded Time Series air temperature data can be accessed at https://crudata.uea.ac.uk/cru/data/hrg/cru_ts4.07/cruts.2304141047.v4.07/tmp/ (accessed on 20 Aug 2023). Land Surface Temperature dataset can be accessed at https://data.ceda.ac.uk/neodc/esacci/land_surface_temperature/data/SSMI_SSMIS/L3C/v2.33/monthly (accessed on 27 Aug 2024). GLEAM Evapotranspiration data can be accessed at https://www.gleam.eu/#downloads (accessed on 19 Mar 2024). Terrestrial Ecoregions dataset can be accessed at https://www.worldwildlife.org/publications/terrestrial-ecoregions-of-the-world (accessed on 5 Sep 2024)

https://doi.org/10.5194/egusphere-2025-762
Preprint. Discussion started: 7 March 2025
© Author(s) 2025. CC BY 4.0 License.

Author Contributions

SX: Conceptualization, Data curation, Formal analysis, Methodology, Software, Validation, Visualization, Writing - Original Draft, Writing - Review & Editing. **GW**: Conceptualization, Funding acquisition, Investigation, Supervision, Writing - Original Draft, Writing - Review & Editing.

Conflicts of Interest

The authors declare that they have no conflict of interest.

Financial Support

This study was funded by the National Key Research and Development Program of China (2022YFF0801302), the National Natural Science Foundation of China (41930970 and 42077421).

https://doi.org/10.5194/egusphere-2025-762
Preprint. Discussion started: 7 March 2025
© Author(s) 2025. CC BY 4.0 License.

Reference

Adler, R. F., and Coauthors, 2003: The Version-2 Global Precipitation Climatology Project (GPCP) Monthly Precipitation Analysis (1979–Present). *Journal of Hydrometeorology*, **4,** 1147-1167.

Berauer, B. J., and Coauthors, 2019: Low resistance of montane and alpine grasslands to abrupt changes in temperature and precipitation regimes. *Arctic, Antarctic, and Alpine Research*, **51,** 215-231.

Browne, W. J., and D. Draper, 2006: A comparison of Bayesian and likelihood-based methods for fitting multilevel models.

Bürkner, P.-C., 2017: brms : An R Package for Bayesian Multilevel Models Using Stan. *Journal of Statistical Software*, **80**.

Buxbaum, C. A. Z., and K. Vanderbilt, 2007: Soil heterogeneity and the distribution of desert and steppe plant species across a desert-grassland ecotone. *Journal of Arid Environments*, **69,** 617-632.

Cammalleri, C., C. De Michele, and A. Toreti, 2024: Exploring the joint probability of precipitation and soil moisture over Europe using copulas. *Hydrol. Earth Syst. Sci.*, **28,** 103-115.

Cook, B. I., G. B. Bonan, and S. Levis, 2006: Soil Moisture Feedbacks to Precipitation in Southern Africa. *Journal of Climate*, **19,** 4198-4206.

Donat, M., A. Lowry, L. Alexander, P. O'Gorman, and N. Maher, 2017: Addendum: More extreme precipitation in the world's dry and wet regions. *Nature Climate Change*, **7,** 154-158.

Drager, A. J., L. D. Grant, and S. C. van den Heever, 2022: A Nonmonotonic Precipitation Response to Changes in Soil Moisture in the Presence of Vegetation. *Journal of Hydrometeorology*, **23,** 1095-1111.

Feldman, A. F., and Coauthors, 2024: Large global-scale vegetation sensitivity to daily rainfall variability. *Nature*, **636,** 380-384.

Graham Emily, B., A. Garayburu-Caruso Vanessa, R. Wu, J. Zheng, R. McClure, and D. Jones Gerrad, 2024: Genomic fingerprints of the world's soil ecosystems. *mSystems*, **9,** e01112-01123.

Gu, C., and Coauthors, 2021: Discrepant responses between evapotranspiration- and transpiration-based ecosystem water use efficiency to interannual precipitation fluctuations. *Agricultural and Forest Meteorology*, **303,** 108385.

Haghighi, E., D. J. Short Gianotti, R. Akbar, G. D. Salvucci, and D. Entekhabi, 2018: Soil and Atmospheric Controls on the Land Surface Energy Balance: A Generalized Framework for Distinguishing Moisture-Limited and Energy-Limited Evaporation Regimes. *Water Resources Research*,

https://doi.org/10.5194/egusphere-2025-762
Preprint. Discussion started: 7 March 2025
© Author(s) 2025. CC BY 4.0 License.

54, 1831-1851.

Harris, I., T. J. Osborn, P. Jones, and D. Lister, 2020: Version 4 of the CRU TS monthly high-resolution gridded multivariate climate dataset. *Scientific Data*, **7,** 109.

He, L., J. Guo, W. Yang, Q. Jiang, L. Chen, and K. Tang, 2023: Multifaceted responses of vegetation to average and extreme climate change over global drylands. *Science of The Total Environment*, **858,** 159942.

Hollmann, R., and Coauthors, 2013: The ESA Climate Change Initiative: Satellite Data Records for Essential Climate Variables. *Bulletin of the American Meteorological Society*, **94,** 1541-1552.

Huffman, G. J., and D. T. Bolvin, 2013: Version 1.2 GPCP one-degree daily precipitation data set documentation. *NASA Goddard Space Flight Center Rep*.

Jafarov, E. E., E. T. Coon, D. R. Harp, C. J. Wilson, S. L. Painter, A. L. Atchley, and V. E. Romanovsky, 2018: Modeling the role of preferential snow accumulation in through talik development and hillslope groundwater flow in a transitional permafrost landscape. *Environmental Research Letters*, **13,** 105006.

Joaquín Muñoz-Sabater, E. D., Anna Agustí-Panareda, Clément Albergel, Gabriele Arduini, Gianpaolo Balsamo, Souhail Boussetta, Margarita Choulga, Shaun Harrigan, Hans Hersbach, Brecht Martens, Diego G. Miralles, María Piles, Nemesio J. Rodríguez-Fernández, Ervin Zsoter, Carlo Buontempo, and Jean-Noël Thépaut, 2021: ERA5-Land: a state-of-the-art global reanalysis dataset for land applications. *Earth Syst. Sci. Data*, **13,** 4349–4383.

Knapp, A. K., and Coauthors, 2008: Consequences of more extreme precipitation regimes for terrestrial ecosystems. *Bioscience*, **58,** 811-821.

Koster, R. D., Z. C. Guo, R. Q. Yang, P. A. Dirmeyer, K. Mitchell, and M. J. Puma, 2009: On the Nature of Soil Moisture in Land Surface Models. *Journal of Climate*, **22,** 4322-4335.

Koukoula, M., C. S. Schwartz, E. I. Nikolopoulos, and E. N. Anagnostou, 2021: Understanding the Impact of Soil Moisture on Precipitation Under Different Climate and Meteorological Conditions: A Numerical Sensitivity Study Over the CONUS. *Journal of Geophysical Research: Atmospheres*, **126,** e2021JD035096.

Lamprecht, A., P. R. Semenchuk, K. Steinbauer, M. Winkler, and H. Pauli, 2018: Climate change leads to accelerated transformation of high-elevation vegetation in the central Alps. *New Phytologist*, **220,** 447-459.

https://doi.org/10.5194/egusphere-2025-762
Preprint. Discussion started: 7 March 2025
© Author(s) 2025. CC BY 4.0 License.

Li, W., and Coauthors, 2022: Widespread increasing vegetation sensitivity to soil moisture. *Nature Communications*, **13**.

Lockwood, M., G. Worboys, and A. Kothari, 2006: *Managing Protected Areas: A Global Guide.*

Lv, P. F., H. F. Hao, and G. C. Wu, 2023: Differences in Global Precipitation Regimes between Land and Ocean Areas Based on the GPM IMERG Product. *Remote Sensing*, **15**.

Ma, S., T. Zhou, A. Dai, and Z. Han, 2015: Observed Changes in the Distributions of Daily Precipitation Frequency and Amount over China from 1960 to 2013. *Journal of Climate*, **28,** 6960-6978.

Mao, Y., G. Wu, G. Xu, and K. Wang, 2022: Reduction in Precipitation Seasonality in China from 1960 to 2018. *Journal of Climate*, **35,** 227-248.

McColl, K. A., S. H. Alemohammad, R. Akbar, A. G. Konings, S. Yueh, and D. Entekhabi, 2017: The global distribution and dynamics of surface soil moisture. *Nature Geoscience*, **10,** 100-+.

McDonald, G. C., 2009: Ridge regression. *WIREs Computational Statistics*, **1,** 93-100.

Miralles, D. G., T. R. H. Holmes, R. A. M. De Jeu, J. H. Gash, A. G. C. A. Meesters, and A. J. Dolman, 2011: Global land-surface evaporation estimated from satellite-based observations. *Hydrol. Earth Syst. Sci.*, **15,** 453-469.

Muñoz Sabater, J., 2019: ERA5-Land hourly data from 1950 to present. Copernicus Climate Change Service (C3S) Climate Data Store (CDS).

Myhre, G., and Coauthors, 2019: Frequency of extreme precipitation increases extensively with event rareness under global warming. *Scientific Reports*, **9,** 16063.

Nelsen, R. B., 2005: 14 - Copulas and quasi-copulas: An introduction to their properties and applications. *Logical, Algebraic, Analytic and Probabilistic Aspects of Triangular Norms*, E. P. Klement, and R. Mesiar, Eds., Elsevier Science B.V., 391-413.

Olson, D., and E. Dinerstein, 1998: The Global 200: A Representation Approach to Conserving the Earth's Most Biologically Valuable Ecoregions. *Conservation Biology*, **12,** 502-515.

Olson, D. M., and Coauthors, 2001: Terrestrial Ecoregions of the World: A New Map of Life on Earth: A new global map of terrestrial ecoregions provides an innovative tool for conserving biodiversity. *BioScience*, **51,** 933-938.

Pepin, N. C., and Coauthors, 2022: Climate Changes and Their Elevational Patterns in the Mountains of the World. *Reviews of Geophysics*, **60,** e2020RG000730.

https://doi.org/10.5194/egusphere-2025-762
Preprint. Discussion started: 7 March 2025
© Author(s) 2025. CC BY 4.0 License.

Prior, L. D., D. Eamus, and G. A. Duff, 1997: Seasonal and Diurnal Patterns of Carbon Assimilation, Stomatal Conductance and Leaf Water Potential in <emph type="2">Eucalyptus tetrodonta</emph> Saplings in a Wet–Dry Savanna in Northern Australia. *Australian Journal of Botany*, **45,** 241-258.

Qiao, L., Z. Zuo, R. Zhang, S. Piao, D. Xiao, and K. Zhang, 2023: Soil moisture-atmosphere coupling accelerates global warming. *Nature communications*, **14,** 4908-4908.

Sala, O., A. Austin, and L. Vivanco, 2001: Temperate Grassland and Shrubland Ecosystems. 627-635.

Sala, O. E., and W. K. Lauenroth, 1985: Root Profiles and the Ecological Effect of Light Rainshowers in Arid and Semiarid Regions. *The American Midland Naturalist*, **114,** 406-408.

Scholes, R. J., and B. H. Walker, 1993: *An African savanna: synthesis of the Nylsvley study.*

shen, S., and Coauthors, 2018: Persistence and Corresponding Time Scales of Soil Moisture Dynamics During Summer in the Babao River Basin, Northwest China. *Journal of Geophysical Research: Atmospheres*, **123,** 8936-8948.

Shen, Z., M. Hua, J. Lu, C. Zhang, and J. Fang, 2016: Response of soil moisture to precipitation in the valley mountain Lhasa, Tibet. *China Rural. Water Hydropower*, **10,** 104-107.

Siebielec, S., G. Siebielec, A. Klimkowicz-Pawlas, A. Gałązka, J. Grządziel, and T. Stuczyński, 2020: Impact of water stress on microbial community and activity in sandy and loamy soils. *Agronomy*, **10,** 1429.

Stocker, B. D., S. J. Tumber-Dávila, A. G. Konings, M. C. Anderson, C. Hain, and R. B. Jackson, 2023: Global patterns of water storage in the rooting zones of vegetation. *Nature Geoscience*, **16,** 250-256.

Straffelini, E., J. Luo, and P. Tarolli, 2024: Climate change is threatening mountain grasslands and their cultural ecosystem services. *CATENA*, **237,** 107802.

Szutu, D. J., and S. A. Papuga, 2019: Year-Round Transpiration Dynamics Linked With Deep Soil Moisture in a Warm Desert Shrubland. *Water Resources Research*, **55,** 5679-5695.

Taylor, C. M., R. A. M. de Jeu, F. Guichard, P. P. Harris, and W. A. Dorigo, 2012: Afternoon rain more likely over drier soils. *Nature*, **489,** 423-426.

Tomlinson, K. W., L. Poorter, F. J. Sterck, F. Borghetti, D. Ward, S. de Bie, and F. van Langevelde, 2013: Leaf adaptations of evergreen and deciduous trees of semi-arid and humid savannas on three continents. *Journal of Ecology*, **101,** 430-440.

Vereecken, H., J. A. Huisman, H. Bogena, J. Vanderborght, J. A. Vrugt, and J. W. Hopmans, 2008: On

https://doi.org/10.5194/egusphere-2025-762
Preprint. Discussion started: 7 March 2025
© Author(s) 2025. CC BY 4.0 License.

the value of soil moisture measurements in vadose zone hydrology: A review. *Water Resources Research*, **44**.

Vidana Gamage, D. N., A. Biswas, and I. B. Strachan, 2020: Scale and location dependent time stability of soil water storage in a maize cropped field. *CATENA*, **188,** 104420.

Walker, D. A., and Coauthors, 2016: Circumpolar Arctic vegetation: a hierarchic review and roadmap toward an internationally consistent approach to survey, archive and classify tundra plot data. *Environmental Research Letters*, **11,** 055005.

Wang, J., D. Liu, P. Ciais, and J. Penuelas, 2022: Decreasing rainfall frequency contributes to earlier leaf onset in northern ecosystems. *Nature Climate Change*, **12,** 386-+.

Wild, B., and Coauthors, 2022: VODCA2GPP – a new, global, long-term (1988–2020) gross primary production dataset from microwave remote sensing. *Earth Syst. Sci. Data*, **14,** 1063-1085.

Wu, G., Y. Li, S. Qin, Y. Mao, and K. Wang, 2021: Precipitation unevenness in gauge observations and eight reanalyses from 1979 to 2018 over China. *Journal of Climate*, **34,** 9797–9810.

Wullschleger, S., and P. Hanson, 2006: Sensitivity of canopy transpiration to altered precipitation in an upland oak forest: evidence from a long-term field manipulation study. *Global Change Biology*, **12,** 97-109.

Xiao, T., P. Li, W. Fei, and J. Wang, 2024: Effects of vegetation roots on the structure and hydraulic properties of soils: A perspective review. *Science of The Total Environment*, **906,** 167524.

Xue, S.-Y., and Coauthors, 2021: Changes in different land cover areas and NDVI values in northern latitudes from 1982 to 2015. *Advances in Climate Change Research*, **12,** 456-465.

Xue, S., and G. Wu, 2023: Sensitivities of Vegetation Gross Primary Production to Precipitation Frequency in the Northern Hemisphere from 1982 to 2015. *Remote Sensing*, **16,** 21.

Xue, S., and G. Wu, 2024: Causal inference of root zone soil moisture performance in drought. *Agricultural Water Management*, **305,** 109123.

Yadav Brijesh, K., S. Mathur, and A. Siebel Maarten, 2009: Soil Moisture Dynamics Modeling Considering the Root Compensation Mechanism for Water Uptake by Plants. *Journal of Hydrologic Engineering*, **14,** 913-922.

Yang, L., G. Sun, L. Zhi, and J. Zhao, 2018: Negative soil moisture-precipitation feedback in dry and wet regions. *Scientific Reports*, **8,** 4026.

https://doi.org/10.5194/egusphere-2025-762
Preprint. Discussion started: 7 March 2025
© Author(s) 2025. CC BY 4.0 License.

Zhang, P., P. Xiao, W. Yao, G. Liu, and W. Sun, 2020: Profile distribution of soil moisture response to precipitation on the Pisha sandstone hillslopes of China. *Scientific Reports*, **10,** 9136.

Zhang, W., T. Zhou, and P. Wu, 2024: Anthropogenic amplification of precipitation variability over the past century. *Science*, **385,** 427-432.

Zhou, S., and Coauthors, 2021: Soil moisture-atmosphere feedbacks mitigate declining water availability in drylands. *Nature Climate Change*, **11,** 274-274.

Zhu, Q., X. Nie, X. Zhou, K. Liao, and H. Li, 2014: Soil moisture response to rainfall at different topographic positions along a mixed land-use hillslope. *Catena*, **119,** 61-70.